C. Sudhakar, N. Bhaskar Reddy, B. Vasu, V. Ramachandra Prasad / International Journal of Engineering Research and Applications (IJERA) ISSN: 2248-9622 www.ijera.com
Vol. 2, Issue5, September- October 2012, pp.2080-2095

Thermophoresis Effect On Unsteady Free Convection Heat And Mass Transfer In A Walters-B Fluid Past A Semi Infinite Plate

C. Sudhakar*, N. Bhaskar Reddy*, #B. Vasu, V. Ramachandra Prasad****
*Department of Mathematics, Sri Venkateswara University, Tirupati, A.P, India
** Department of Mathematics, Madanapalle Institute of Technology and Sciences, Madanapalle-517325, India.

ABSTRACT

The effect of thermophoresis particle deposition on unsteady free convective, heat and mass transfer in a viscoelastic fluid along a semi-infinite vertical plate is investigated. The Walters-B liquid model is employed to simulate medical creams and other rheological liquids encountered in biotechnology and chemical engineering. The dimensionless unsteady, coupled and non-linear partial differential conservation equations for the boundary layer regime are solved by an efficient, accurate and unconditionally stable finite difference scheme of the Crank-Nicolson type. The behavior of velocity, temperature and concentration within the boundary layer has been studied for variations in the Prandtl number (Pr), viscoelasticity parameter (□), Schmidt number (Sc), buoyancy ration parameter (N) and thermophoretic parameter (τ). The local skin-friction, Nusselt number and Sherwood number are also presented and analyzed graphically. It is observed that, an increase in the thermophoretic parameter (τ) decelerates the velocity as well as concentration andaccelerates temperature. In addition, the effect of the thermophoresis is also discussed for the case of Newtonian fluid.

Key words: Finite difference method,semi-infinite vertical plate, Thermophoresis effect, Walters-B fluid, unsteady flow.

1. INTRODUCTION

Prediction of particle transport in non-isothermal gas flow is important in studying the erosion process in combustors and heat exchangers, the particle behavior in dust collectors and the fabrications of optical waveguide and semiconductor device and so on. Environmental regulations on small particles have also become more stringent due to concerns about atmospheric pollution.

When a temperature gradient is established in gas, small particles suspended in the gas migrate in the direction of decreasing temperature. The phenomenon, called thermophoresis, occurs because gas molecules colliding on one side of a particle have different average velocities from those on the other side due to the temperature gradient. Hence when a cold wall is placed in the hot particle-laden gas flow, the thermophoretic deposition plays an important role in a variety of applications such as the production of ceramic powders in high temperature aerosol flow reactors, the production of optical fiber performs by the modified chemical vapor deposition (MCVD) process and in a polymer separation. Thermophoresis is considered to be important for particles of 10 m in radius and temperature gradient of the order of 5 K/mm. Walker et al. [1] calculated the deposition efficiency of small particles due to thermophoresis in a laminar tube flow. The effect of wall suction and thermophoresis on aerosol-particle deposition from a laminar boundary layer on a flat plate was studied by Mills et al. [2]. Ye et al. [3] analyzed the thermophoretic effect of particle deposition on a free standing semiconductor wafer in a clean room. Thakurta et al. [4] computed numerically the deposition rate of small particles on the wall of a turbulent channel flow using the direct numerical simulation (DNS). Clusters transport and deposition processes under the effects of thermophoresis were investigated numerically in terms of thermal plasma deposition processes by Han and Yoshida [5]. In their analysis, they found that the thickness of the concentration boundary layer was significantly suppressed by the thermophoretic force and it was concluded that the effect of thermophoresis plays a more dominant role than that of diffusion. Recently, Alam et al. [6] investigated numerically the effect of thermophoresis on surface deposition flux on hydromagnetic free convective heat mass transfer flow along a semi- infinite permeable inclined flat plate considering heat generation. Their results show that thermophoresis increases surface mass flux significantly. Recently, Postalnicu [7] has analyzed the effect of thermophoresis particle deposition in free convection boundary layer from a horizontal flat plate embedded in porous medium.

The study of heat and mass transfer in non-Newtonian fluids is of great interest in many operations in the chemical and process engineering industries including coaxial mixers, blood oxygenators [8], milk processing [9], steady-state tubular reactors and capillary column inverse gas chromatography devices mixing mechanism bubble-drop formation processes [10] dissolution processes and cloud transport phenomena. Many liquids possess complex shear-stress relationships which

deviate significantly from the Newtonian (Navier-Stokes) model. External thermal convection flows in such fluids have been studied extensively using mathematical and numerical models and often employ boundary-layer theory. Many geometrical configurations have been addressed including flat plates, channels, cones, spheres, wedges, inclined planes and wavy surfaces. Non-Newtonian heat transfer studies have included power-law fluid models [11-13] i.e. shear-thinning and shear thickening fluids, simple viscoelastic fluids [14, 15], Criminale-Ericksen-Fibley viscoelastic fluids [16], Johnson-Segalman rheological fluids [17], Bingham yield stress fluids [18], second grade (Reiner-Rivlin) viscoselastic fluids [19] third grade viscoelastic fluids [20], micropolar fluids [21] and bi-viscosity rheological fluids [22]. Viscoelastic properties can enhance or depress heat transfer rates, depending upon the kinematic characteristics of the flow field under consideration and the direction of heat transfer. The Walters-B viscoelastic model [23] was developed to simulate viscous fluids possessing short memory elastic effects and can simulate accurately many complex polymeric, biotechnological and tribological fluids. The Walters-B model has therefore been studied extensively in many flow problems. Soundalegkar and Puri[24] presented one of the first mathematical investigations for such a fluid considering the oscillatory two-dimensional viscoelastic flow along an infinite porous wall, showing that an increase in the Walters elasticity parameter and the frequency parameter reduces the phase of the skin-friction. Roy and Chaudhury [25] investigated heat transfer in Walters-B viscoelastic flow along a plane wall with periodic suction using a perturbation method including viscous dissipation effects. Raptis and Takhar [26] studied flat plate thermal convection boundary layer flow of a Walters-B fluid using numerical shooting quadrature. Chang et al [27] analyzed the unsteady buoyancy-driven flow and species diffusion in a Walters-B viscoelastic flow along a vertical plate with transpiration effects. They showed that the flow is accelerated with a rise in viscoelasticity parameter with both time and distances close to the plate surface and that increasing Schmidt number suppresses both velocity and concentration in time whereas increasing species Grashof number (buoyancy parameter) accelerates flow through time. Hydrodynamic stability studies of Walters-B viscoelastic fluids were communicated by Sharma and Rana [28] for the rotating porous media suspension regime and by Sharma et al [29] for Rayleigh-Taylor flow in a porous medium. Chaudhary and Jain [30] studied the Hall current and cross-flow effects on free and forced Walters-B viscoelastic convection flow with thermal radiative flux effects. Mahapatra et al [31] examined the steady two-dimensional stagnation-point flow of a Walters-B fluid along a flat deformable stretching surface. They found that a boundary layer is generated formed when the inviscid free-stream velocity exceeds the stretching velocity of the surface and the flow is accelerated with increasing magnetic field. This study also identified the presence of an inverted boundary layer when the surface stretching velocity exceeds the velocity of the free stream and showed that for this scenario the flow is decelerated with increasing magnetic field. Rajagopal et al [32] obtained exact solutions for the combined nonsimilar hydromagnetic flow, heat, and mass transfer phenomena in a conducting viscoelastic Walters-B fluid percolating a porous regime adjacent to a stretching sheet with heat generation, viscous dissipation and wall mass flux effects, using confluent hypergeometricfunctions for different thermal boundary conditions at the wall.

Steady free convection heat and mass transfer flow of an incompressible viscous fluid past an infinite or semi-infinite vertical plate is studied since long because of its technological importance. Pohlhausen [33], Somers [34] and Mathers et al. [35] were the first to study it for a flow past a semi-infinite vertical plate by different methods. But the first systematic study of mass transfer effects on free convection flow past a semi-infinite vertical plate was presented by Gebhart and pera [36] who presented a similarity solution to this problem and introduced a parameter N which is a measure of relative importance of chemical and thermal diffusion causing a density difference that drives the flow. Soundalgekar and Ganesan [37] studied transient free convective flow past a semi-infinite vertical flat plate with mass transfer by using Crank–Nicolson finite difference method. In their analysis they observed that, an increase in *N* leads to an increase in the velocity but a decrease in the temperature and concentration. Prasad et al. [38] studied Radiation effects on MHD unsteady free convection flow with mass transfer past a vertical plate with variable surface temperature and concentration Owing to the significance of this problem in chemical and medical biotechnological processing (e.g. medical cream manufacture).

Therefore the objective of the present paper is to investigate the effect of thermophoresis on an unsteady free convective heat and mass transfer flow past a semi infinite vertical plate using the robust Walters-B viscoelastic rheologicctal material model.A Crank-Nicolson finite difference scheme is utilized to solve the unsteady dimensionless, transformed velocity, thermal and concentration boundary layer equations in the vicinity of the vertical plate. The present problem has to the author' knowledge not appeared thus far in the literature. Another motivation of the study is to er observed high heat transfer performance commonly attributed to extensional investigate thestresses in viscoelastic boundary layers [25]

2. CONSTITUTIVE EQUATIONS FOR THE WALTERS-B VISCOELASTIC FLUID

Walters [23] has developed a physically accurate and mathematically amenable model for the rheological equation of state of a viscoelastic fluid of short memory. This model has been shown to capture the characteristics of actual viscoelastic polymer solutions, hydrocarbons, paints and other chemical engineering fluids. The Walters-B model generates highly non-linear flow equations which are an order higher than the classical Navier-Stokes (Newtonian) equations. It also incorporates elastic properties of the fluid which are important in extensional behavior of polymers. The constitute equations for a Walters-B liquid in tensorial form may be presented as follows:

$$p_{ik} = -pg_{ik} + p_{ik}^{*} \quad (1)$$

$$p_{ik}^{*} = 2\int_{-\infty}^{1} \psi\left(t-t^{*}\right) e^{(1)}{}_{ik}\left(t^{*}\right) dt^{*} \quad (2)$$

$$\psi\left(t-t^{*}\right) = \int_{0}^{\infty} \frac{N(\tau)}{\tau} e\left(-\left(t-t^{*}\right)/\tau\right) d\tau \quad (3)$$

where p_{ik} is the stress tensor, p is arbitrary isotropic pressure, g_{ik} is the metric tensor of a fixed coordinate system xi, $e_{ik}^{(1)}$ is the rate of strain tensor and $N(\tau)$ is the distribution function of relaxation times, . The following generalized form of (2) has been shown by Walters [23] to be valid for all classes of motion and stress.

$$p_{ik}^{*}(x,t) = 2\int_{-\infty}^{1} \psi\left(t-t^{*}\right) \frac{\partial x'}{\partial x^{*m} \partial x^{*r}} e^{(1)mr}\left(x^{*}t^{*}\right) dt^{*} \quad (4)$$

in which $x_i^{*} = x_i^{*}\left(x,t,t^{*}\right)$ denotes the position at time t* of the element which is instantaneously at the position, *xi*, at time, *t*. Liquids obeying the relations (1) and (4) are of the Walters-B' type. For such fluids with short memory i.e. low relaxation times, equation (4) may be simplified to:

$$p^{*ik}(x,t) = 2\eta_0 e^{(1)ik} - 2k_0 \frac{\partial e^{(1)ik}}{\partial t} \quad (5)$$

in which $\eta_0 = \int_0^{\infty} N(\tau) d\tau$ defines the limiting Walters-B' viscosity at low shear rates, $k_0 = \int_0^{\infty} \tau N(\tau) d\tau$ is the Walters-B' viscoelasticity parameter and $\frac{\partial}{\partial t}$ is the convected time derivative. This rheological model is very versatile and robust and provides a relatively simple mathematical formulation which is easily incorporated into boundary layer theory for engineering applications [25, 26].

3. MATHEMATICAL MODEL:

An unsteady two-dimensional laminar free convective flow of a viscoelastic fluid past a semi-infinite vertical plate is considered. The x-axis is taken along the plate in the upward direction and the y-axis is taken normal to it. The physical model is shown in Fig.1a.

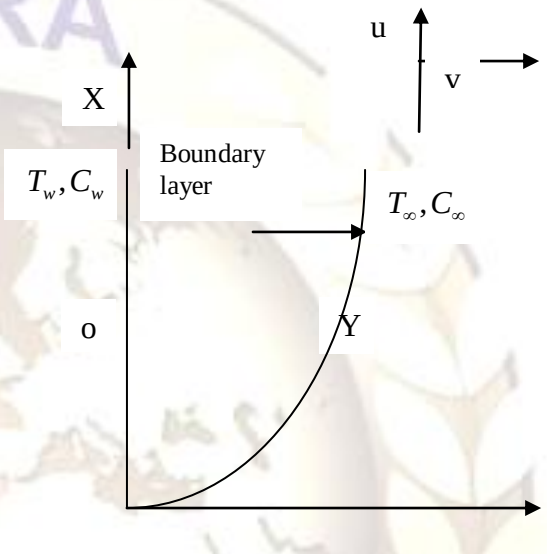

Fig.1a. Flow configuration and coordinate system

Initially, it is assumed that the plate and the fluid are at the same temperature T_∞' and concentration level C_∞' everywhere in the fluid. At time, t' >0, Also, the temperature of the plate and the concentration level near the plate are raised to T_w' and C_w' respectively and are maintained constantly thereafter. It is assumed that the concentration C' of the diffusing species in the binary mixture is very less in comparison to the other chemical species, which are present, and hence the Soret and Dufour effects are negligible. It is also assumed that there is no chemical reaction between the diffusing species and the fluid. Then, under the above assumptions, the governing boundary layer equations with Boussinesq's approximation are

$$\frac{\partial u}{\partial x} + \frac{\partial v}{\partial y} = 0 \quad (6)$$

$$\frac{\partial u}{\partial t'}+u\frac{\partial u}{\partial x}+v\frac{\partial u}{\partial y}=g\beta\left(T'-T'_\infty\right)+g\beta^*\left(C'-C'_\infty\right)+ \nu\frac{\partial^2 u}{\partial y^2}-k_0\frac{\partial^3 u}{\partial y^2\partial t'} \quad (7)$$

$$\frac{\partial T'}{\partial t'}+u\frac{\partial T'}{\partial x}+v\frac{\partial T'}{\partial y}=\frac{k}{\rho c_p}\frac{\partial^2 T'}{\partial y^2} \quad (8)$$

$$\frac{\partial C'}{\partial t'}+u\frac{\partial C'}{\partial x}+v\frac{\partial C'}{\partial y}=D\frac{\partial^2 C'}{\partial y^2}-\frac{\partial}{\partial y}\left(c'v_t\right) \quad (9)$$

The initial and boundary conditions are

$$t'\le 0: u=0, v=0, T'=T'_\infty, C'=C'_\infty 0$$
$$t'>0: u=0, v=0, T'=T'_w, C'=C'_w \ \ at \ \ y=0$$
$$u=0, T'=T'_\infty, C'=C'_\infty \ \ at \ \ x=0$$
$$u\to 0, T'\to T'_\infty, C'\to C'_\infty \ \ as \ \ y- \quad (10)$$

Where u, v are velocity components in x and y directions respectively, t' - the time, g – the acceleration due to gravity, β - the volumetric coefficient of thermal expansion, β^* - the volumetric coefficient of expansion with concentration, T' -the temperature of the fluid in the boundary layer, C' -the species concentration in the boundary layer, T'_w - the wall temperature, T'_∞ - the free stream temperature far away from the plate, C'_w - the concentration at the plate, C'_∞ - the free stream concentration in fluid far away from the plate, ν - the kinematic viscosity, α - the thermal diffusivity, ρ - the density of the fluid and D - the species diffusion coefficient.

In the equation (4), the thermophoretic velocity V_t was given by Talbot et al. [39] as

$$V_T=-k\nu\frac{\nabla T}{T_w}=-\frac{k\nu}{T_w}\frac{\partial T}{\partial y}$$

Where T_w is some reference temperature, the value of kv represents the thermophoretic diffusivity, and k is the thermophoretic coefficient which ranges in value from 0.2 to 1.2 as indicated by Batchelor and Shen [40] and is defined from the theory of Talbot et al [39] by

$$k=\frac{2C_s(\lambda_g/\lambda_p+C_tK_n)\left[1+K_n(C_1+C_2e^{-C_s/K_n})\right]}{(1+3C_mK_n)\left(1+2\lambda_g/\lambda_p+2C_tK_n\right)}$$

A thermophoretic parameter τ can be defined (see Mills et al [2] and Tsai [41]) as follows;

$$\tau=\frac{k\left(T_w-T_\infty\right)}{T_0}$$

Typical values of □ are 0.01, 0.05 and 0.1 corresponding to approximate values of $k\left(T_w-T_\infty\right)$ equal to 3.15 and 30 k for a reference temperature of T_0 =300 k.

On introducing the following non-dimensional quantities

$$X=\frac{x}{L}, Y=\frac{yGr^{1/4}}{L}, U=\frac{uLGr^{-1/2}}{\nu},$$
$$T=\frac{T'-T'_\infty}{T'_w-T'_\infty}, C=\frac{C'-C'_\infty}{C'_w-C'_\infty}, t'=\frac{tL^2}{\nu}Gr^{-1/2}, \quad (11)$$
$$N=\frac{\beta^*(C'_w-C'_\infty)}{\beta(T'_w-T'_\infty)}, \Gamma=\frac{k_0Gr^{1/2}}{L^2},$$
$$Gr=\frac{\nu g\beta(T'_w-T'_\infty)}{{u_0}^3},$$
$$\Pr=\frac{\nu}{\alpha}, Sc=\frac{\nu}{D}, \tau=\frac{kL\left(T'_w-T'_\infty\right)}{T_w}$$

Equations (6), (7), (8), (9) and (10) are reduced to the following non-dimensional form

$$\frac{\partial U}{\partial X}+\frac{\partial U}{\partial Y}=0 \quad (12)$$

$$\frac{\partial U}{\partial t}+U\frac{\partial U}{\partial X}+V\frac{\partial U}{\partial Y}=\frac{\partial^2 U}{\partial Y^2}+T+NC-\Gamma\frac{\partial^3 U}{\partial Y^2\partial t} \quad (13)$$

$$\frac{\partial T}{\partial t}+U\frac{\partial T}{\partial X}+V\frac{\partial T}{\partial Y}=\frac{1}{\Pr}\frac{\partial^2 T}{\partial Y^2} \quad (14)$$

$$\frac{\partial C}{\partial t}+U\frac{\partial C}{\partial X}+V\frac{\partial C}{\partial Y}=\frac{1}{Sc}\frac{\partial^2 C}{\partial Y^2}+ \frac{\tau}{Gr^{1/4}}\left[\frac{\partial C}{\partial Y}\frac{\partial T}{\partial Y}+C\frac{\partial^2 T}{\partial Y^2}\right] \quad (15)$$

The corresponding initial and boundary conditions are

$$t\le 0: U=0, V=0, T=0, C=0$$
$$t>0: \ U=0, \ V=0, \ T=1, C=1 \ \ at \ \ Y=0,$$
$$U=0, V=0, C=0 \ \ as \ \ X=0$$
$$U\to 0, V\to 0, C\to 0 \ \ as \ \ Y\to\infty \quad (16)$$

Where Gr is the thermal Grashof number, Pr is the fluid Prandtl number, Sc is the Schmidt number, N is the buoyancy ratio parameter, □ is the viscoelastic parameter and □ is the thermophoretic parameter.

To obtain an estimate of flow dynamics at the barrier boundary, we also define several important

rate functions at Y = 0. These are the dimensionless wall shear stress function, i.e. local skin friction function, the local Nusselt number (dimensionless temperature gradient) and the local Sherwood number (dimensionless species, i.e. contaminant transfer gradient) are computed with the following mathematical expressions [48]

$$\tau_X = Gr^{3/4}\left(\frac{\partial U}{\partial Y}\right)_{Y=0}, \quad Nu_x = \frac{-XGr^{1/4}\left(\frac{\partial T}{\partial Y}\right)_{Y=0}}{T_{Y=0}},$$

$$Sh_X = \frac{-XGr^{1/4}\left(\frac{\partial C}{\partial Y}\right)_{Y=0}}{C_{Y=0}} \qquad (17)$$

We note that the dimensionless model defined by Equations (12) to (15) under conditions (16) reduces to Newtonian flow in the case of vanishing viscoelasticity i.e. when □ = 0

4.NUMERICAL SOLUTION

In order to solve these unsteady, non-linear coupled equations (12) to (15) under the conditions (16), an implicit finite difference scheme of Crank-Nicolson type has been employed. This method was originally developed for heat conduction problems [42]. It has been extensively developed and remains one of the most reliable procedures for solving partial differential equation systems. It is unconditionally stable. It utilizes a central differencing procedure for space and is an implicit method. The partial differential terms are converted to difference equations and the resulting algebraic problem is solved using a triadiagonal matrix algorithm. For transient problems a trapezoidal rule is utilized and provides second-order convergence. The Crank-Nicolson Method (CNM) scheme has been applied to a rich spectrum of complex multiphysical flows. Kafousias and Daskalakis [43] have employed the CNM to analyze the hydromagnetic natural convection Stokes flow for air and water. Edirisinghe [44] has studied efficiently the heat transfer in solidification of ceramic-polymer injection moulds with CNFDM. Sayed-Ahmed [45] has analyzed the laminar dissipative non-Newtonian heat transfer in the entrance region of a square duct using CNDFM. Nassab [46] has obtained CNFDM solutions for the unsteady gas convection flow in a porous medium with thermal radiation effects using the Schuster-Schwartzchild two-flux model. Prasad et al [47] studied the combined transient heat and mass transfer from a vertical plate with thermal radiation effects using the CNM method. The CNM method works well with boundary-layer flows. The finite difference equations corresponding to equations (12) to (15) are discretized using CNM as follows

$$\frac{1}{4\Delta x}U_{i,j-1}^{n+1} - U_{i-1,j-1}^{n+1} + U_{i,j}^{n+1} - U_{i-1,j}^{n+1} + U_{i,j-1}^{n} - U_{i-1,j-1}^{n} + U_{i,j}^{n} - U_{i-1,j}^{n} + \frac{V_{i,j}^{n+1} - V_{i,j-1}^{n+1} + V_{i,j}^{n} - V_{i,j-1}^{n}}{2\Delta y} = 0 \qquad (18)$$

$$\frac{U_{i,j}^{n+1} - U_{i,j}^{n}}{\Delta t} + U_{i,j}^{n}\frac{U_{i,j}^{n+1} - U_{i-1,j}^{n+1} + U_{i,j}^{n} - U_{i-1,j}^{n}}{2\Delta x} + V_{i,j}^{n}\frac{U_{i,j+1}^{n+1} - U_{i,j-1}^{n+1} + U_{i,j+1}^{n} - U_{i,j-1}^{n}}{4\Delta y} = \frac{U_{i,j-1}^{n+1} - 2U_{i,j}^{n+1} + U_{i,j+1}^{n+1} + U_{i,j-1}^{n} - 2U_{i,j}^{n} + U_{i,j+1}^{n}}{2(\Delta y)^2} - \Gamma\frac{U_{i,j-1}^{n+1} - 2U_{i,j}^{n+1} + U_{i,j+1}^{n+1} + U_{i,j-1}^{n} - 2U_{i,j}^{n} + U_{i,j+1}^{n}}{2(\Delta y)^2\Delta t} + Gr^{-1/4}\frac{T_{i,j}^{n+1} + T_{i,j}^{n}}{2} + N\frac{C_{i,j}^{n+1} + C_{i,j}^{n}}{2} \qquad (19)$$

$$\frac{T_{i,j}^{n+1} - T_{i,j}^{n}}{\Delta t} + U_{i,j}^{n}\frac{T_{i,j}^{n+1} - T_{i-1,j}^{n+1} + T_{i,j}^{n} - T_{i-1,j}^{n}}{2\Delta x} + V_{i,j}^{n}\frac{T_{i,j+1}^{n+1} - T_{i,j-1}^{n+1} + T_{i,j+1}^{n} - T_{i,j-1}^{n}}{4\Delta y} = \frac{1}{\Pr}\frac{T_{i,j-1}^{n+1} - 2T_{i,j}^{n+1} + T_{i,j+1}^{n+1} + T_{i,j-1}^{n} - 2T_{i,j}^{n} + T_{i,j+1}^{n}}{2(\Delta y)^2} \qquad (20)$$

$$\frac{C_{i,j}^{n+1} - C_{i,j}^{n}}{\Delta t} + U_{i,j}^{n}\frac{C_{i,j}^{n+1} - C_{i-1,j}^{n+1} + C_{i,j}^{n} - C_{i-1,j}^{n}}{2\Delta x} + V_{i,j}^{n}\frac{C_{i,j+1}^{n+1} - C_{i,j-1}^{n+1} + C_{i,j+1}^{n} - C_{i,j-1}^{n}}{4\Delta y} = \frac{1}{Sc}\frac{C_{i,j-1}^{n+1} - 2C_{i,j}^{n+1} + C_{i,j+1}^{n+1} + C_{i,j-1}^{n} - 2C_{i,j}^{n} + C_{i,j+1}^{n}}{2(\Delta y)^2} + \frac{\tau}{Gr^{1/4}}\left(\frac{C_{i,j+1}^{n+1} - C_{i,j-1}^{n+1} + C_{i,j+1}^{n} - C_{i,j-1}^{n}}{4\Delta y}\right)\left(\frac{T_{i,j+1}^{n+1} - T_{i,j-1}^{n+1} + T_{i,j+1}^{n} - T_{i,j-1}^{n}}{4\Delta y}\right) + \frac{\tau}{Gr^{1/4}}C_{i,j}^{n}\frac{T_{i,j-1}^{n+1} - 2T_{i,j}^{n+1} + T_{i,j+1}^{n+1} + T_{i,j-1}^{n} - 2T_{i,j}^{n} + T_{i,j+1}^{n}}{2(\Delta y)^2} \qquad (21)$$

Here the region of integration is considered as a rectangle with $X_{\max} = 1, Y_{\max} = 14$ and where $Y_{\max}$ corresponds to Y□ □ □ □ which lies well outside both the momentum and thermal boundary layers. The maximum of Y was chosen as 14, after some preliminary numerical experiments such that the last two boundary conditions of (19) were satisfied within the tolerance limit 10^{-5}. The mesh sizes have been fixed as□□□ X□ □ □ □ □ □ □ □ Y□ □ □ □ □ □ with time step □*t*□ □ 0.01. The computations are executed initially by reducing the spatial mesh sizes by 50% in one direction, and later in both directions by 50%. The results are compared. It is observed that, in all the cases, the results differ only in the fifth decimal place. Hence, the choice of the mesh sizes is verified as extremely efficient. The coefficients of $U_{i,j}^{k}$ *and* $V_{i,j}^{k}$,appearing in the finite difference equations are treated as constant at any one-time step. Here *i* designates the grid point along the *X*-direction, *j* along the *Y*-direction and *k* in the time variable, t. The values of *U, V, T* and *C* are known at all grid points when *t = 0* from the initial conditions. The computations for *U, V, T* and *C* at a time level (k + 1), using the values at previous time level k are carried out as follows. The finite-difference equation (21) at every internal nodal point on a particular *i*□ level constitutes a tri-diagonal system of equations and is solved by Thomas algorithm as discussed in Carnahan et al. [45]. Thus, the values of *C* are known at every nodal point at a particular *i* at $(k+1)^{th}$ time level. Similarly, the values of *U* and *T* are calculated from equations (19), (20) respectively, and finally the values of *V* are calculated explicitly by using equation (18) at every nodal point on a particular *i* □ □ level at $(k+1)^{th}$ time level. In a similar manner, computations are carried out by moving along *i* -direction. After computing values corresponding to each *i* at a time level, the values at the next time level are determined in a similar manner. Computations are repeated until steady state is reached. The steady state solution is assumed to have been reached when the absolute difference between the values of the velocity *U*, temperature *T*, as well as concentration *C* at two consecutive time steps are less than 10^{-5} at all grid points. The scheme is unconditionally stable. The local truncation error is $O(\Delta t^2 + \Delta X^2 + \Delta Y^2)$ □ and it tends to zero as □*t*, □ X, □ and □*Y*□ □ tend to zero. It follows that the CNM scheme is compatible. Stability and compatibility ensure the convergence.

5.RESULTS AND DISCUSSION

In order to get a physical insight into the problem, a parametric study is carried out to illustrate the effect of various governing thermophysical parameters on the velocity, temparature, concentration, skin-friction, Nusselt number and Sherwood number are shown in figures and tables.

In figures 2(a) to 2(c) we have presented the variation of velocity U, temparature T and concentration C versus (Y) with collective effects of thermophoretic parameter (□) at X = 0 for opposing flow (N<0). In case of Newtonian fluids (□ = 0), an increase in □ from 0.0 through 0.5 to maximum value of 1.0 as depicted in figure 2(a) for opposing flow (N < 0) . Clearly enhances the velocity U which ascends sharply and peaks in close vicinity to the plate surface (Y=0). With increasing distance from the plate wall however the velocity U is adversely affected by increasing thermophoretic effect i.e. the flow is decelerated. Therefore close to the plate surface the flow velocity is maximized for the case of□ □ □ □ □ □ But this trend is reversed as we progress further into the boundary layer regime. The switchover in behavior corresponds to approximately Y =3.5, with increasing velocity profiles decay smoothly to zero in the free stream at the edge of the boundary layer. The opposite effect is caused by an increase in time.A rise in □ from 6.36, 7.73 to 10.00 causes a decrease in flow velocity U near the wall in this case the maximum velocity arises for the least time progressed.With more passage of time t = 10.00 the flow is decelerated.Again there is a reverse in the response at Y =3.5, and thereafter velocity is maximized with the greatest value of time. A similar response is observed for the non-Newtonian fluid ($\Gamma \neq 0$), but clearly enhances the velocity very sharply and peaks highly in close vicinity to the plate surface compared in case of Newtonian fluid.

In figure 2(b), in case of Newtonian fluids (□ =0) and non-Newtonian fluids ($\Gamma \neq 0$), the thermophoretic parameter □ is seen to increase temperature throughout the bounder layer.All profiles increases from the maximum at the wall to zero in the free stream. The graphs show therefore that increasing thermophoretic parameter heated the flow. With progression of time, however the temperature T is consistently enhanced i.e. the fluid is cool as time progress.

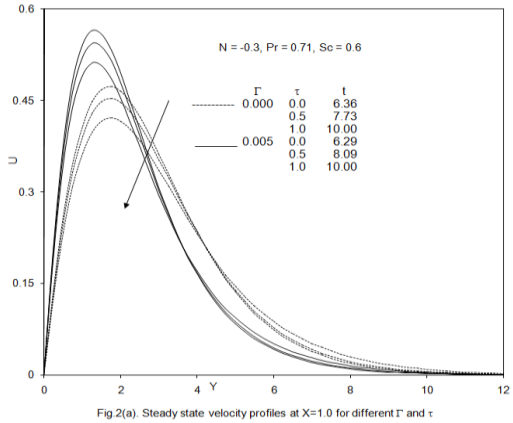

Fig.2(a). Steady state velocity profiles at X=1.0 for different Γ and τ

In figure 2(c) theopposite response is observed for the concentration field C. In case of Newtonian fluids (□ =0) and non-Newtonian fluids ($\Gamma \neq 0$), the thermophoretic parameter □ □ increases, the concentration throughout the boundary layer regime (0<Y<14) decreased.

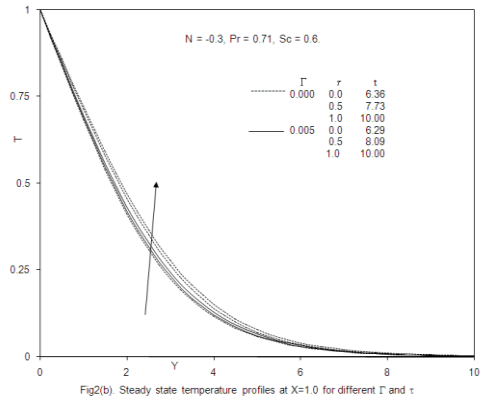

Fig2(b). Steady state temperature profiles at X=1.0 for different Γ and τ

In figures 3(a) to 3(c) we have presented the variation of velocity U, temparature T and concentration C versus (Y) with collective effects of thermophoretic parameter□ □ at X = 0 for aiding flow. In case of Newtonian fluids (□ = 0), an increase in □ from 0.0 through 0.5 to maximum value of 1.0 as depicted in figure 3(a) for aiding flow (N>0). Clearly enhances the velocity U which ascends sharply and peaks in close vicinity to the plate surface (Y=0). With increasing distance from the plate wall however the velocity U is adversely affected by increasing thermophoretic effect i.e. theflow is decelerated. Therefore close to the plate surface the flow velocity is maximized for the case of □ □ □ □ □ But this trend is reversed as we progress further into the boundary layer regime.

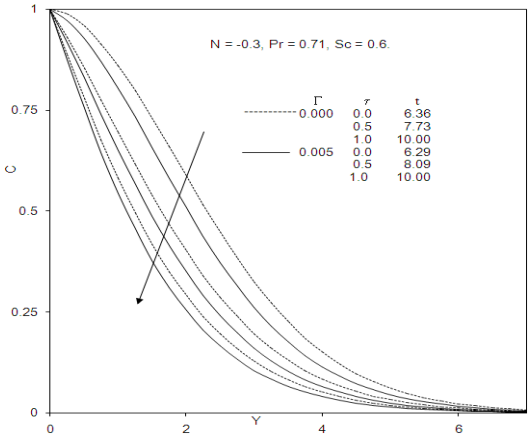

Fig.2(c). Steady state concentration profiles at X=1.0 for different Γ and τ

The switchover in behavior corresponds to approximately Y =3.5, with increasing velocity profiles decay smoothly to zero in the free stream at the edge of the boundary layer.The opposite effect is caused by an increase in time. A rise in time t from 6.36, 7.73 to 10.00 causes a decrease in flow

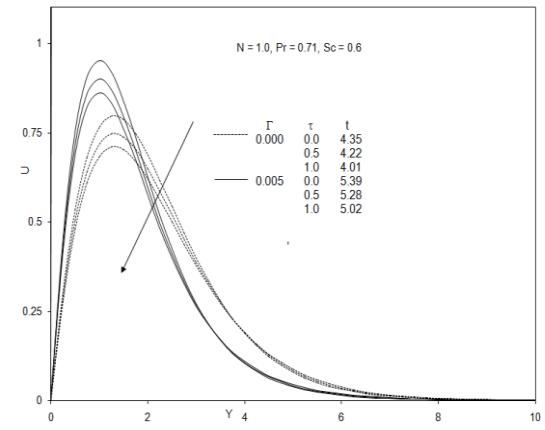

Fig.3(a). Steady state velocity profiles at X=1.0 for different Γ and τ

velocity U near the wall in this case the maximum velocity arises for the least time progressed.With more passage of time t = 10.00 the flow is decelerated. Again there is a reverse in the response at Y =3.5, and thereafter velocity is maximized with the greatest value of time. A similar response is observed for the non-Newtonian fluid ($\Gamma \neq 0$), but clearly enhances the velocity very sharply and peaks highly in close vicinity to the plate surface compared in case of Newtonian fluid.

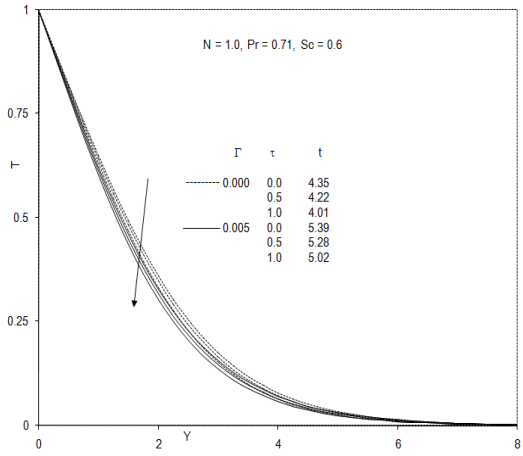

Fig.3(b). Steady state temperature profiles at X=1.0 for different Γ and τ

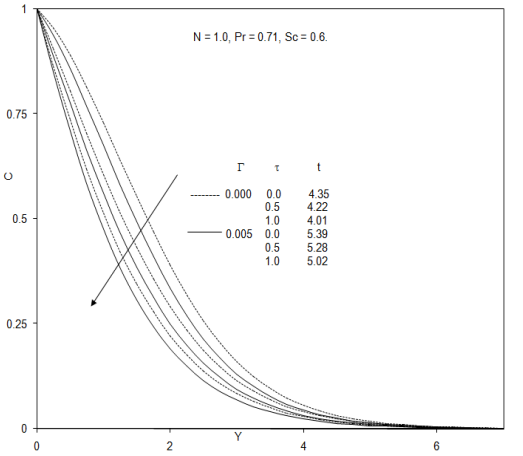

Fig.3(c). Steady state concentration profiles at X=1.0 for different Γ and τ

In figure 3(b), in case of Newtonian fluids (□ =0) and non-Newtonian fluids ($\Gamma \neq 0$), the thermophoretic parameter □ is seen to decrease temperature throughout the bounder layer. All profiles decreases from the maximum at the wall to zero in the free stream. The graphs show therefore that increasing thermophoretic parameter cools the flow. With increasing of time t, the temperature T is consistently enhanced i.e. the fluid is heated as time progress.

In figure 3(c) a similar response is observed for the concentration field C. In case of Newtonian fluids (□ =0) and non-Newtonian fluids ($\Gamma \neq 0$), the thermophoretic parameter □ increases, the concentration throughout the boundary layer regime (0<Y<14) decreased. All profiles decreases from the maximum at the wall to zero in the free stream.

Figures 4(a) to 4(c) illustrate the effect of Prandtl number (Pr), Viscoelastic parameter (□) and time t on velocity (U), temperature (T) and concentration (C) without thermophoretic effect (□ =0) at X=1.0.Pr defines the ratio of momentum diffusivity (□) to thermal diffusivity. In case of air based solvents i.ePr = 0.71, an increase in □ from 0.000, 0.003 and the maximum value of 0.005 as depicted in figure 4(a), clearly enhances the velocity U which ascends sharply and peaks in close vicinity to the plate surface (Y=0),with increasing distance from the plate wall the velocity U is adversely affected by increasing viscoelasticity i.e. the flow is decelerated. Therefore close to the plate surface the flow velocity is maximized for the case ofnon-Newtonian fluid($\Gamma \neq 0$). The switchover in behavior corresponds to approximately Y=2.

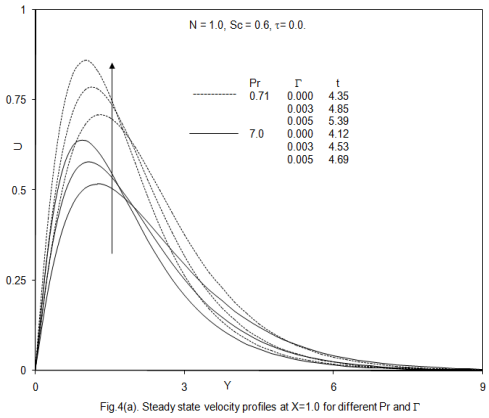

Fig.4(a). Steady state velocity profiles at X=1.0 for different Pr and Γ

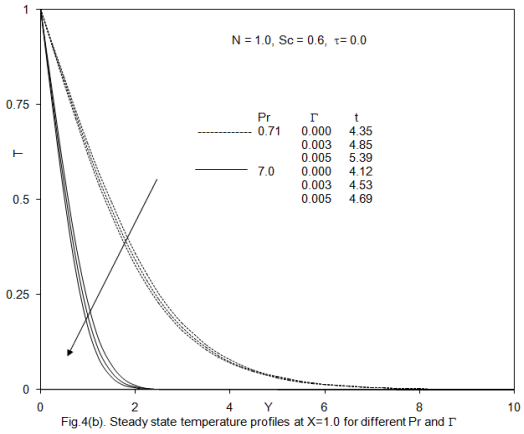

Fig.4(b). Steady state temperature profiles at X=1.0 for different Pr and Γ

With increasing Y, velocity profiles decay smoothly to zero in the free stream at the edge of theboundary layer. Pr<1 physically corresponds to cases where heat diffuses faster than momentum. In the case of water based solvents i.e. Pr = 7.0, a similar response is observed for the velocity field in figure 4(a).

In figure 4(b), in case of air based solvents i.e. Pr = 0.71, an increase in viscoelasticity □ increasing from 0.000, 0.003 to 0.005, temperature T is markedly reduced throughout the boundary layer. In case of water based solvents i.e. Pr = 7.0 also a similar response is observed, but it is very closed to the plate surface. The descent is increasingly sharper near the plate surface for higher Pr values a more gradual monotonic decay is witnessed smaller Pr values in this case, cause a thinner thermal boundary layer thickness and more uniform temperature distributions across the boundary layer. Smaller Pr fluids possess higher thermal conductivities so that heat can diffuse away

from the plate surface faster than for higher Pr fluids (thicker boundary layers). Our computations show that a rise in Pr depresses the temperature function, a result constant with numerous other studies on coupled heat and mass transfer. For the case of Pr = 1, thermal and velocity boundary layer thickness are equal.

A similar response is observed for the concentration field C in figure 4(c). In both cases Pr = 0.71 and Pr = 7.0, when □ increasing from 0.000, 0.003 to 0.005, concentration C also reduced throughout the boundary layer regime (0<Y<14). All profiles decreases from the maximum at the wall to zero in the free stream.

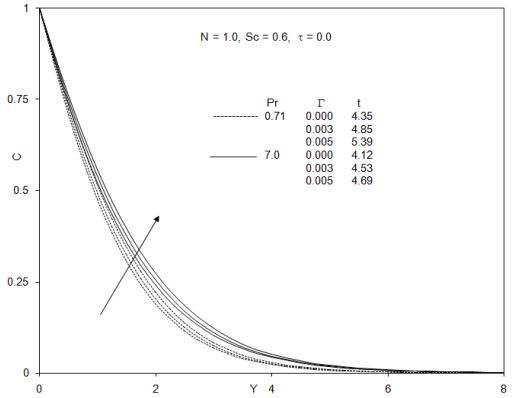

Fig.4(c). Steady state concentration profiles at X=1.0 for different Pr and Γ

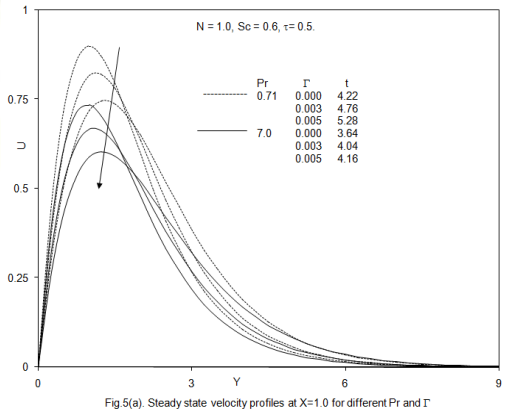

Fig.5(a). Steady state velocity profiles at X=1.0 for different Pr and Γ

Figures 5(a) to 5(c) illustrate the effect of Prandtl number (Pr), Viscoelastic parameter (□) and time t on velocity U, temperature T and concentration C with thermophoretic effect (□ = 0.5) at X=1.0. In case of air based solvents i.ePr = 0.71, an increase in □ from 0.000, 0.003 and the maximum value of 0.005 as depicted in figure 5(a), clearly enhances the velocity U which ascends sharply and peaks in close vicinity to the plate surface (Y=0). With increasing Y, velocity profiles decay smoothly to zero in the free stream at the edge of the boundary layer.

In figure 5(b), in case of air based solvents i.e. Pr = 0.71, an increase in viscoelasticity □ increasing from 0.000, 0.003 to 0.005, temperature T is markedly reduced throughout the boundary layer. In case of water based solvents i.e. Pr = 7.0 also a similar response is observed, but it is very closed to the plate surface. A similar response is observed for the concentration field C in figure 5(c).In both cases Pr = 0.71 and Pr = 7.0, when □ increasing from 0.000, 0.003 to 0.005, concentration C also reduced throughout the boundary layer regime (0<Y<14). All profiles decreases from the maximum at the wall to zero in the free stream.

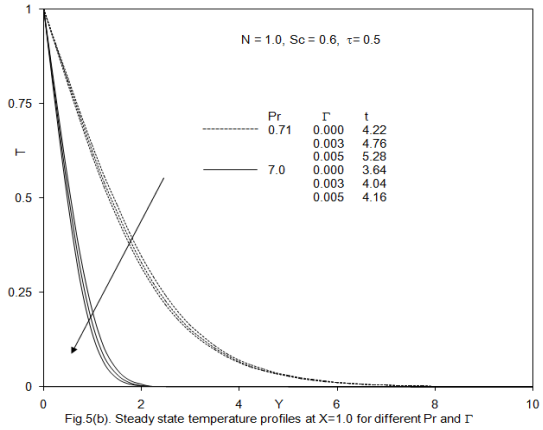

Fig.5(b). Steady state temperature profiles at X=1.0 for different Pr and Γ

Figures 6(a) to 6(c) depict the distributions of velocity U, temperature T and concentration C versus coordinate (Y) for various Schmidtnumbers (Sc) with collective effects of thermophoretic parameter (□) in case of Newtonian fluids (□ =0) and time (t), close to the leading edge at X = 1.0, are shown. Correspond to Schmidt number Sc=0.6 an increase in □ □ from 0.0 through 0.5 to 1.0 as depicted in figure 6(a), clearly enhances the velocity U which ascends sharply and peaks in close vicinity to the plate surface (Y=0). With increasing distance from the plate wall however the velocity U is adversely affected by increasing thermophoretic effect i.e. the flow is decelerated.

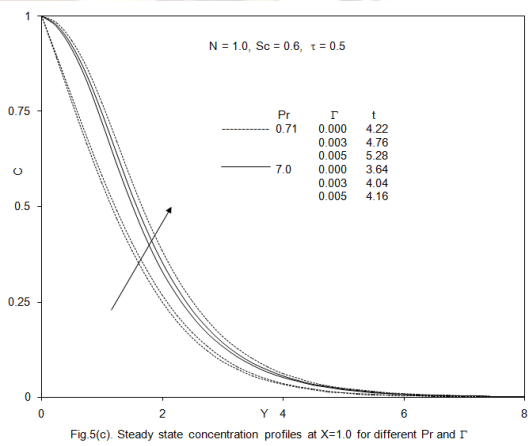

Fig.5(c). Steady state concentration profiles at X=1.0 for different Pr and Γ

Therefore close to the plate surface the flow velocity is maximized for the case of □ □ □ □ □ But this trend is reversed as we progress further into the boundary layer regime. The switchover in behavior corresponds to

approximately Y =3.5, with increasing velocity profiles decay smoothly to zero in the free stream at the edge of the boundary layer.A similar response is observed in case of Schmidt number Sc=2.0 also.

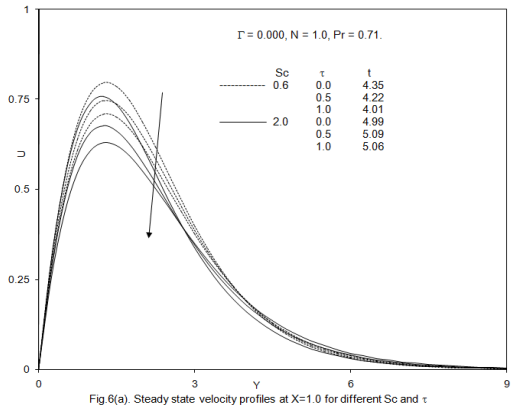

Fig.6(a). Steady state velocity profiles at X=1.0 for different Sc and τ

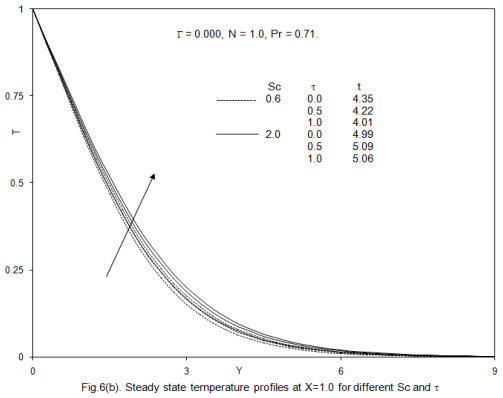

Fig.6(b). Steady state temperature profiles at X=1.0 for different Sc and τ

With higher Sc values the gradient of velocity profiles is lesser prior to the peak velocity but greater after the peak.

In figure 6(b), in case of Newtonian fluids (□ =0) and for Schmidt number Sc=0.6, and 2.0 the increasing in thermophoretic parameter □ is seen to decrease the temperature throughout the bounder layer. All profiles decreases from the maximum at the wall to zero in the free stream. The graphs show therefore that decreasing thermophoretic parameter cools the flow. With progression of time, however the temperature T is consistently enhanced i.e. the fluid is heated as time progress.

In figure 6(c) a similar response is observed for the concentration field C. In case of Newtonian fluids (□ =0) and for Schmidt number Sc=0.6, and 2.0, the increasing in thermophoretic parameter □ □ increases the concentration throughout the boundary layer regime (0<Y<14). All profiles increases from the maximum at the wall to zero in the free stream. Sc defines the ratio of momentum diffusivity (□) to molecular diffusivity (*D*). For Sc<1, species will diffuse much faster than momentum so that

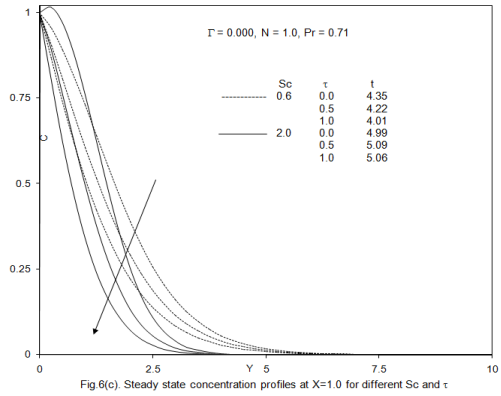

Fig.6(c). Steady state concentration profiles at X=1.0 for different Sc and τ

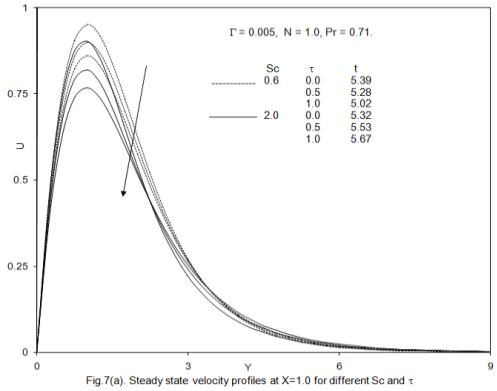

Fig.7(a). Steady state velocity profiles at X=1.0 for different Sc and τ

maximum concentrations will be associated with this case (Sc = 0.6).For Sc > 1, momentum will diffuse faster than species causing progressively lower concentration values. With a increase in molecular diffusivity concentration boundary layer thickness is therefore increased. For the special case of *Sc* = 1, the species diffuses at the same rate as momentum in the viscoelastic fluid. Both concentration and boundary layer thicknesses are the same for this case. An increase in Schmidt number effectively depresses concentration values in the boundary layer regime since higher *Sc* values will physically manifest in a decrease of molecular diffusivity (*D*) of the viscoelastic fluid i.e. a reduction in the rate of mass diffusion. Lower *Sc* values will exert the reverse influence since they correspond to higher molecular diffusivities. Concentration boundary layer thickness is therefore considerably greater for *Sc* = 0.6 than for *Sc* = 2.0.

Figures 7(a) to 7(c) depict the distributions of velocity U, temperature T and concentration C versus coordinate (Y) for various Schmidt numbers (Sc) with collective effects of thermophoretic parameter (□) in case of non-Newtonian fluids($\Gamma \neq 0$) and time (t), close to the leading edge at X = 1.0, are shown. Correspond to Schmidt number Sc=0.6 an

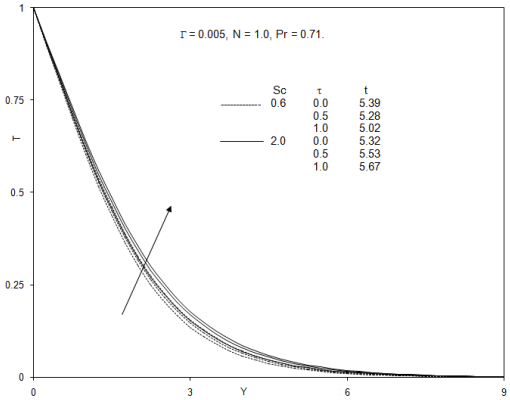

Fig.7(b). Steady state temperature profiles at X=1.0 for different Sc and τ

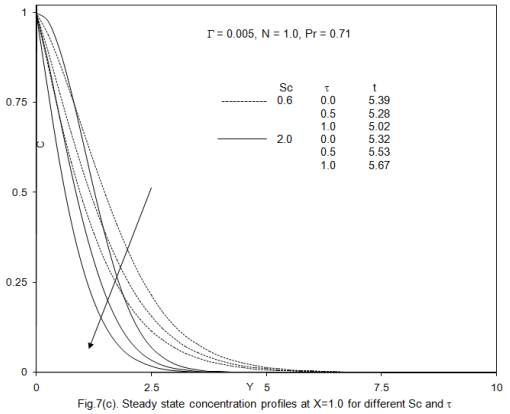

Fig.7(c). Steady state concentration profiles at X=1.0 for different Sc and τ

increase in □□ from 0.0 through 0.5 to 1.0 as depicted in figure 7(a),clearly enhances the velocity U which ascends sharply and peaks in close vicinity to the plate surface (Y=0). With increasing distance from the plate wall however the velocity U is adversely affected by increasing thermophoretic effect i.e. the flow is decelerated. Therefore close to the plate surface the flow velocity is maximized for the case of □ □ □ □ □ But this trend is reversed as we progress further into the boundary layer regime. The switchover in behavior corresponds to approximately Y =3.5, with increasing velocity profiles decay smoothly to zero in the free stream at the edge of the boundary layer. A similar response is observed in case of Schmidt number Sc=2.0 also. All profiles descend smoothly to zero in the free stream. With higher Sc values the gradient of velocity profiles is lesser prior to the peak velocity but greater after the peak.

In figure 7(b), in case of non-Newtonian fluids ($\Gamma \neq 0$) and for Schmidt number Sc=0.6, and 2.0 the increasing in thermophoretic parameter □ is seen to decrease the temperature throughout the bounder layer. All profiles decreases from the maximum at the wall to zero in the free stream. The graphs show therefore that decreasing thermophoretic parameter cools the flow. With progression of time, however the temperature T is consistently enhanced i.e. the fluid is heated as time progress.

In figure 7(c) a similar response is observed for the concentration field C. In case of non-Newtonian fluids ($\Gamma \neq 0$) and for Schmidt number Sc=0.6, and 2.0, the increasing in thermophoretic parameter □ □ increases the concentration throughout the boundary layer regime (0<Y<14). All profiles increases from the maximum at the wall to zero in the free stream. Sc defines the ratio of momentum diffusivity (n) to molecular diffusivity (*D*). For Sc<1, species will diffuse much faster than momentum so that maximum concentrations will be associated with this case (Sc = 0.6). For Sc > 1, momentum will diffuse faster than species causing progressively lower concentration values. With a increase in molecular diffusivity concentration boundary layer thickness is therefore increased. For the special case of *Sc* = 1, the species diffuses at the same rate as momentum in the viscoelastic fluid. Both concentration and boundary layer thicknesses are the same for this case. An increase in Schmidt number effectivelydepresses concentration values in the boundary layer regime since higher *Sc* values will physically manifest in a decrease of molecular diffusivity (*D*) of the viscoelastic fluid i.e. a reduction in the rate of mass diffusion. Lower *Sc* values will exert the reverse influence since they correspond to higher molecular diffusivities. Concentration boundary layer thickness is therefore considerably greater for *Sc* = 0.6 than for *Sc* = 2.0.

Figures 8a to 8c present the effects of buoyancy ratio parameter, *N* on U, T and C profiles. The maximum time elapse to the steady state scenario accompanies the only negative value of *N* i.e. *N* = -0.5. For *N* = 0 and then increasingly positive values of *N* up to 5.0, the time taken, *t*, is steadily reduced. As such the presence of aidingbuoyancy forces (both thermal and species buoyancy force acting in unison) serves to stabilize the transient flow regime. The parameter $N = \dfrac{\beta^*\left(C'_w - C'_\infty\right)}{\beta\left(T'_w - T'_\infty\right)}$ and expresses the ratio of the species (mass diffusion) buoyancy force to the thermal (heat diffusion) buoyancy force. When *N* = 0 the species buoyancy term, *NC* vanishes and the momentum boundary layer equation (13) is de-coupled from the species diffusion (concentration) boundary layer equation (15). Thermal buoyancy does not vanish in the momentum equation (13) since the term *T* is not affected by the buoyancy ratio.

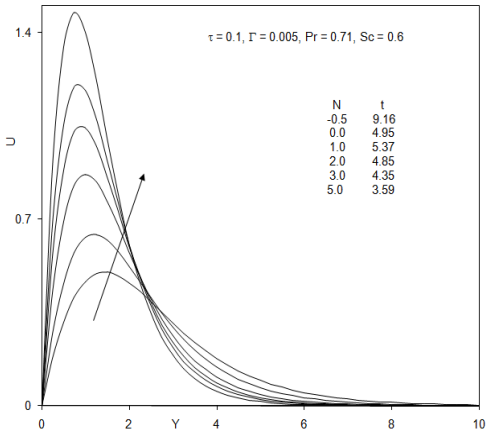

Fig.8(a). Steady state velocity profiles at X=1.0 for different N.

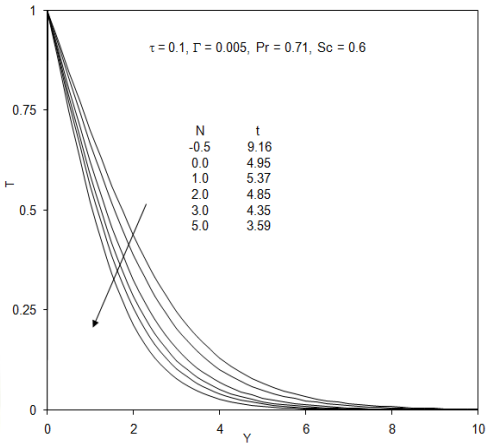

Fig.8(b). Steady state temperature profiles at X=1.0 for different N.

When $N < 0$ we have the case of opposing buoyancy. An increase in N from -0.5, through 0, 1, 2, 3, to 5 clearly accelerates the flow i.e. induces a strong escalation in stream wise velocity, U, close to the wall; thereafter velocities decay to zero in the free stream. At some distance from the plate surface, approximately $Y = 2.0$, there is a cross-over in profiles. Prior to this location the above trends are apparent. However after this point, increasingly positive N values in fact decelerate the flow. Therefore further from the plate surface, negative N i.e. opposing buoyancy is beneficial to the flow regime whereas closer to the plate surface it has a retarding effect. A much more consistent response to a change in the N parameter is observed in figure 8b, where with a rise from -0.5 through 0, 1.0, 2.0, 3.0 to 5.0 (very strong aiding buoyancy case) the temperature throughout the boundary layer is strongly reduced. As with the velocity field (figure 8a), the time required to attain the steady state decreases substantially with a positive increase in N. Aiding (assisting) buoyancy therefore stabilizes the temperature distribution.A similar response is evident for the concentration distribution C, Whichs shown in figure 8c, also decreases with positiveincrease in N but reaches the steady state progressively faster.

In **figures 9a to 9c** the variation of dimensionless local skin friction (surface shear stress), τ_X, Nusselt number (surface heat transfer gradient), Nu_X and the Sherwood number (surface concentration gradient), Sh_X, versus axial coordinate (X) for various viscoelasticity parameters (□) and timetare illustrated.Shear stress is clearly enhanced with increasing viscoelasticity (i.e. stronger elastic effects) i.e. the flow is accelerated, a trend consistent with our earlier computations in figure 9a.

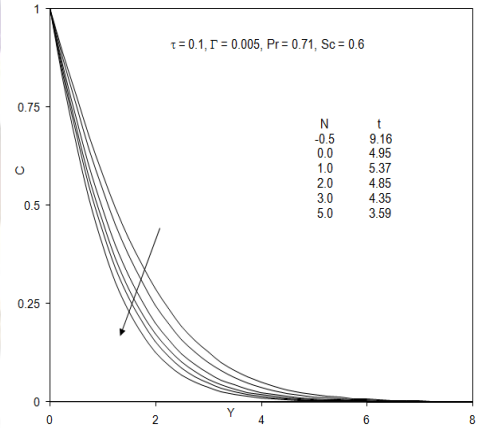

Fig.8(c). Steady state concentration profiles at X=1.0 for different N.

The ascent in shear stress is very rapid from the leading edge ($X = 0$) but more gradual as we progress along the plate surface away from the plane.With an increase in time, t, shear stress, τ_X is increased.Increasing viscoelasticity (□) is observed in figure 9b to enhance local Nusselt number, Nu_X values whereas they areagain increased with greater time.Similarly in figure 9c the local Sherwood number Sh_X

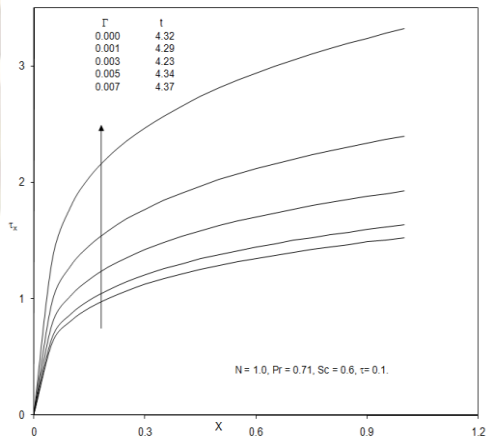

Fig9(a). The local Skin friction results for different Γ

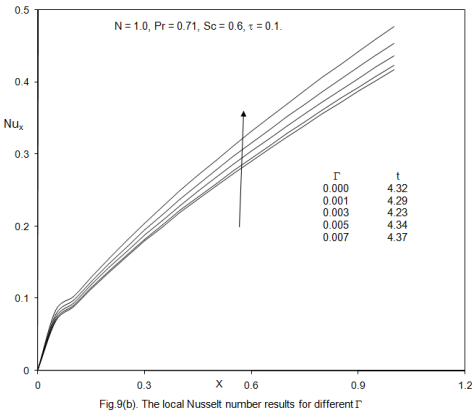

Fig.9(b). The local Nusselt number results for different Γ

values are elevated with an increase in elastic effects i.e. a rise in □ □ from 0 (Newtonian flow) though 0.001, 0.003, 0.005 to 0.007 but depressed slightly with time.

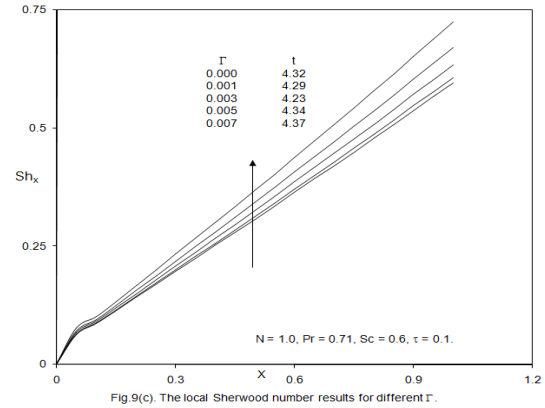

Fig.9(c). The local Sherwood number results for different Γ.

Finally in **figures 10a to 10c** the influence of Thermophoretic parameter and time (t) on τ_X, Nu_X and Sh_X, versus axial coordinate (X) are depicted.

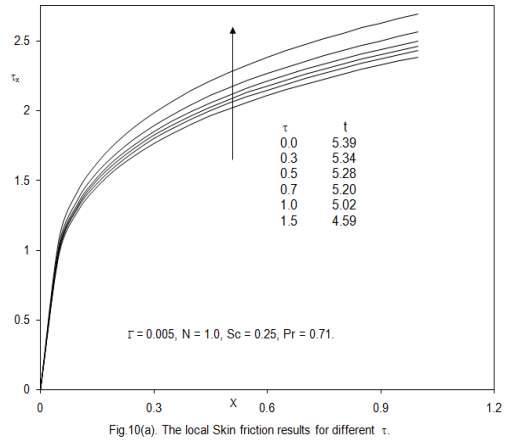

Fig.10(a). The local Skin friction results for different τ.

An increase in □ from 0.0 through 0.3, 0.5, 1.0 to 1.5, strongly increases both τ_X and Nu_X along the entire plate surface i.e. for all X. However with an increase in time (t) both Shear stress and local Nusselt number are enhanced.

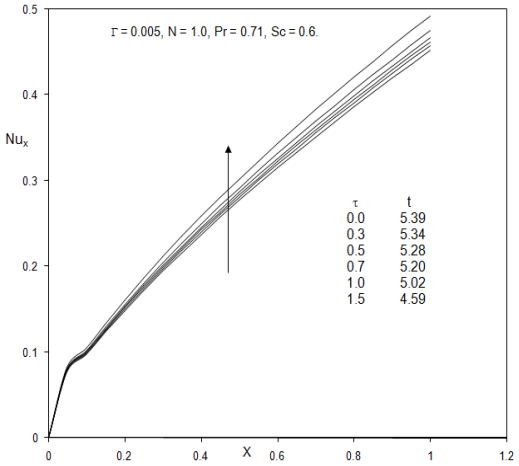

Fig.10(b). The local Nusselt number results for different τ

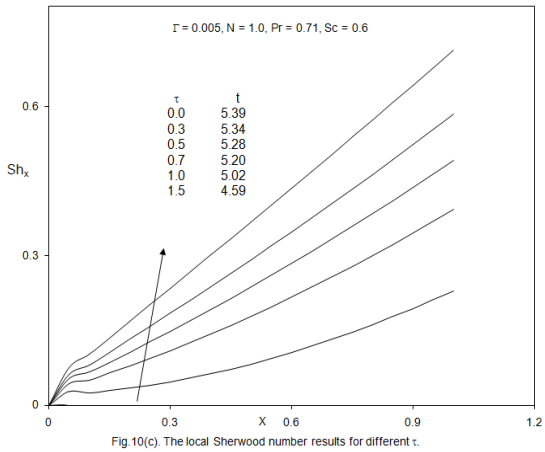

Fig.10(c). The local Sherwood number results for different τ.

With increasing □ values, local Sherwood number, Sh_X, as shown in figure 10c, is boosted considerably along the plate surface;gradients of the profiles are also found to diverge with increasing X values. However an increase in time, t, serves to increase local Sherwood numbers.

6. CONCLUSIONS

A two-dimensional, unsteady laminar incompressible boundary layer model has been presented for the external flow, heat and mass transfer in a viscoelastic buoyancy-driven flow past a semi-infinite vertical plate under the influence of thermophoresis. The Walters-B viscoelastic model has been employed which is valid for short memory polymeric fluids. The dimensionless conservation equations have been solved with the well-tested, robust, highly efficient, implicit Crank Nicolson finite difference numerical method. The present computations have shown that increasing viscoelasticity accelerates the velocity and enhances shear stress (local skin friction), local Nusselt number and local Sherwood number, but reduces

temperature and concentration in the boundary layer.

7. NOMENCLATURE

x, y	coordinates along the plate generator and normal to the generator respectively
u, v	velocity components along the x- and y-directions respectively
g	gravitational acceleration
t□	time
t	dimensionless time
Gr	thermal Grashof number
k_0	Walters-B viscoelasticity parameter
L	reference length
Nu_X	Non-dimensional local Nusselt number
Pr	Prandtl number
T□	temperature
T	dimensionless temperature
C□	concentration
C	dimensionless concentration
D	mass diffusion coefficient
N	Buoyancy ratio number
U, V	dimensionless velocity components along the X- and Y- directions respectively
X, Y	dimensionless spatial coordinates along the plate generator and normal to the generator respectively
Sc	Schmidt number
V_t	thermophoretic velocity
Sh_X	non-dimensional local Sherwood number

Greek symbols

□	thermal diffusivity
□	volumetric thermal expansion coefficient
β^*	volumetric concentration expansion coefficient
□	viscoelastic parameter
τ	thermophoretic parameter
□ □	kinematic viscosity
Δt	dimensionless time-step
ΔX	dimensionless finite difference grid size in X-direction
ΔY	dimensionless finite difference grid size in Y-direction
τ_x	dimensionless local skin-friction

Subscripts

w	condition on the wall
∞	free stream condition

REFERENCES

[1] K.L. Walker, G. M. Homsy, F. T. Geying, thermophoretic deposition of small particles in laminar tube,*Journal of colloid and interface science*,69, 1979, 138-147.

[2] A. F. Mills, X. Hang, F. Ayazi, The effect of wall suction and thermophoresis on aerosol- particle deposition from a laminar boundary layer on a flat plane, *International journal of Heat and Mass Transfer*, 27, 1984, 1110-1113.

[3] Y. Ye, D. Y. H. Pui, B.Y.H.Lia. S.Opiolka, S. Opiolka, S.Blumhorst, H. Fisson, Thermophoretic effect of particle deposition on a free standing semiconductor wafer in a clean room, *journal of Aerosol science*,22(1), 1991, 63-72.

[4] D.G.Thakurta, M. Chen, J.B.Mclaughlim, K.Kontomaris, Tthermophoretic deposition of small particles in a direct numerical simulation of turbulent channel flow, *Internationaljournal of Heat and mass transfer*, 41, 1998, 4167-4182.

[5] P. Han, T. Yoshida, Numerical investigationof thermophoretic effects of cluster transport during thermal plasma deposition process,*Journal of Applied Physics*,91(4), 2002, 1814-1818.

[6] M.S.Alam, M.M. Rahman, M.A.Sattar, Similarity solutions for hydromagnetic free convective heat and mass transfer flow along a semi-infinite permeable inclined flat plate with heat generation and thermophoresis. Nonlinear Anal model control ,12(4), 2007, 433-445.

[7] A Postelnicu, Effects of thermophoresis particle deposition in free convection boundary layer from a horizontal flat plate embedded in a porous medium,*Internationaljournal of Heat and mass transfer*,50, *2007*, 2981-2985.

[8] A. R. Goerke, J. Leung and S. R. Wickramasinghe, Mass and momentum transfer in blood oxygenators, *Chemical Engineering Science*, 57(11), 2002, 2035-2046.

[9] W. Wang and G. Chen, Heat and mass transfer model of dielectric-material-assisted microwave freeze-drying of skim milk with hygroscopic effect, *Chemical Engineering Science*, 60(23), 2005, 6542-6550.

[10] A. B. Jarzebski and J. J. Malinowski, Transient mass and heat transfer from drops or bubbles in slow non-Newtonian flows, *Chemical Engineering Science*, 41(10), 1986,. 2575-2578.

[11] R. PrakashBharti, R.P. Chhabra and V. Eswaran, Effect of blockage on heat transfer from a cylinder to power law liquids, *Chemical Engineering Science*, 62(17), 2007, 4729-4741.

[12] R. Mahalingam, S. F. Chan and J. M. Coulson, Laminar pseudoplastic flow heat transfer with prescribed wall heat flux,

Chemical Engineering Journal, 9(2), 1975, 161-166.

[13] C.Kleinstreuer and T-Y. Wang, Mixed convection heat and surface mass transfer between power-law fluids and rotating permeable bodies, *Chemical Engineering Science*, 44(12), 1989, 2987-2994.

[14] J. L. White and A. B. Metzner, Thermodynamic and heat transport considerations for viscoelastic fluids, *Chemical Engineering Science*, 20(12), 1965, 1055-1062.

[15] A. V. Shenoy and R. A. Mashelkar, Laminar natural convection heat transfer to a viscoelastic fluid, *Chemical Engineering Science*, 33(6), 1978, 769-776.

[16] S. Syrjälä, Laminar flow of viscoelastic fluids in rectangular ducts with heat transfer: A finite element analysis, *International Communication in Heat and Mass Transfer*, 25(2), 1998, 191-204.

[17] T. Hayat, Z. Iqbal, M. Sajid, K. Vajravelu Heat transfer in pipe flow of a Johnson–Segalman fluid, *International Communication in Heat and Mass Transfer*, 35(10), 2008, 1297-1301.

[18] K. J. Hammad and G. C. Vradis, Viscous dissipation and heat transfer in pulsatile flows of a yield-stress fluid, *International Communication in Heat and Mass Transfer*, 23(5), 1996, . 599-612.

[19] O. A. Bég, Takhar H.S., Kumari M. and Nath G., Computational fluid dynamics modelling of buoyancy induced viscoelastic flow in a porous medium with magnetic field, *Internationaljournal of Applied Mechanics Engineering*, 6(1), (2001), 187-210.

[20] R. Bhargava, Rawat S., Takhar. H.S., Bég. O.A and V.R. Prasad, Numerical Study of heat transfer of a third grade viscoelastic fluid in non-Darcy porous media with thermophysical effects, *PhysicaScripta: Proc. Royal Swedish Academy of Sciences*, 77, 2008, 1-11.

[21] O. A. Bég, R. Bhargava, K. Halim and H. S. Takhar, Computational modeling of biomagnetic micropolar blood flow and heat transfer in a two-dimensional non-Darcian porous medium, *Meccanica*, 43, 2008, 391-410.

[22] J. Zueco and O. A. Bég, Network numerical simulation applied to pulsatile non-Newtonian flow through a channel with couple stress and wall mass flux effects, *Internationaljournal of Applied Mathematics and Mechanics*, 5(2), 2009, 1-16.

[23] K. Walters, Non-Newtonian effects in some elastico-viscous liquids whose behaviour at small rates of shear is characterized by a general linear equation of state, *Quarterly Journal of Mechanics and Applied. Mathematics*, 15, 1962, 63-76.

[24] V. M. Soundalgekar and P. Puri On fluctuating flow of an elastico-viscous fluid past an infinite plate with variable suction, *Journal of Fluid Mechanics*, 35(3), 1969, 561-573.

[25] J. S. Roy and N. K. Chaudhury, Heat transfer by laminar flow of an elastico-viscous liquid along a plane wall with periodic suction, *Czechoslovak Journal of Physics*, 30(11) 1980, 1199-1209.

[26] A. A. Raptis and H. S. Takhar, Heat transfer from flow of an elastico-viscous fluid, *International Communication in Heat and Mass Transfer*, 16(2), 1989, 193-197.

[27] T.B. Chang, Bég, O. Anwar, J. Zueco and M. Narahari, Numerical study of transient free convective mass transfer in a Walters-B viscoelastic flow with wall suction, *Journal of Theoretical Applied Mechanics, under review*, 2009.

[28] V.Sharma and G.C.Rana, Thermosolutal instability of Walters' (model B') visco-elastic rotating fluid permeated with suspended particles and variable gravity field in porous medium, *International journal of Applied Mechanics Engineering*, 6(4), 2001, 843-860.

[29] R. C. Sharma, P. Kumar and S. Sharma., Rayleigh-Taylor instability of Walters- B elastico-viscous fluid through porous medium, *International journal of Applied Mechanics Engineering*, 7(2), 2002, 433-444.

[30] R. C. Chaudhary, and P. Jain, Hall effect on MHD mixed convection flow of a viscoelastic fluid past an infinite vertical porous plate with mass transfer and radiation, *Theoretical and Applied Mechanics*, 33(4), 2006, 281-309.

[31] T. Ray Mahapatra, S. Dholey and A. S. Gupta, Momentum and heat transfer in the magnetohydrodynamic stagnation-point flow of a viscoelastic fluid toward a stretching surface, *Meccanica*, 42(3), 2007, 263-272.

[32] K. Rajagopal, P. H. Veena and V. K. Pravin, Nonsimilar Solutions for heat and mass transfer flow in an electrically conducting viscoelastic fluid over a stretching sheet saturated in a porous medium with suction/blowing, *Journal of Porous Media*, 11(2), 2008, 219-230.

[33] E.Pohlhausen, Der Warmeaustrauschzwischenfestenkorpen and FlussigkeitenmitKleinerReibung under

KleinerWarmeleitung, *Journal of Applied Mathematics and Mechanics*, 1, 1921, 115-121.

[34] E.V. Somers, Theoretical considerations of combined thermal and mass transfer from vertical flat plate, *Journal of Applied Mechanics*, 23, 1956, 295-301.

[35] W.G.Mathers, A.J. Madden, and E.L. Piret, Simultaneous heat and mass transfer in free convection, *Industrial and Engineering Chemistry Research*, 49, 1956, 961-968.

[36] B.Gebhart and L.Pera, The nature of vertical natural convection flows resulting from the combined buoyancy effects of thermal and mass diffusion, *International journal of heat and mass transfer*, 14, 1971, 2025-2050.

[37] V.M. Soundalgekar and P.Ganesan, Finite difference analysis of transient free convection with mass transfer on an isothermal vertical flat plate, *International journal of engineering science*, 19, 1981, 757-770.

[38] V. R. Prasad., N. Bhaskar Reddy and Muthucumaraswamy., Radiation effects on MHD unsteady free convection flow with mass transfer past a vertical plate with variable surface temperature and concentration, *Journal of energy, heat and mass transfer*, 31, 2009, 239-260.

[39] L Talbot, R K Cheng, A W Schefer, D R wills, Thermophoresis of particles in a heated boundary layer, *Journal of Fluid Mechanics*, 101, 1980, 737-758.

[40] G K Batchelor, C. Shen, Thermophoretic deposition of particles in gas flowing over cold surface,*Journal of colloid and interface science*, 107, 1985, 21-37.

[41] R Tsai, A simple approach for evaluating the effect of wall suction and thermophoresis on aerosol particle deposition from a laminar flow over a flat plate, *International Communication in Heat and Mass Transfer*, 26, 1999, 249-257.

[42] J. Crank, and P. Nicolson, A practical method for numerical evaluation of solutions of partial differential equations of the heat conduction type, *Proceedings of the Cambridge Philosophical Society*, 43, 1947, 50-67.

[43] N.G. Kafousias and J. Daskalakis, Numerical solution of MHD free-convection flow in the Stokes problem by the Crank-Nicolson method, *Astrophysics and Space Science*, **106(**2), 1984, 381-389.

[44] M.J. Edirisinghe, Computer simulating solidification of ceramic injection moulding formulations, *Journal of Materials Science Letters*, **7**(5), 1988, 509-510.

[45] M.E. Sayed-Ahmed, Laminar heat transfer for thermally developing flow of a Herschel-Bulkley fluid in a square duct, *International Communication in Heat and Mass Transfer*,**27(**7), 2000, 1013-1024.

[46] A.S.G. Nassab, Transient heat transfer characteristics of an energy recovery system using a porous medium, *IMechE Journal of Power and Energy*, **216(**5), 2002, 387-394.

[47] V. R. Prasad, N. Bhaskar Reddy and R. Muthucumaraswamy, Radiation and mass transfer effects on two-dimensional flow past an impulsively started infinite vertical plate, *InternationalJouanal of Thermal Sciences*, 46(12), 2007, 1251-1258.

B. Carnahan, H. A. Luther, J. O. Wilkes, Applied Numerical Methods, John Wiley and Sons, New York, 1969.